Line to Ground Fault Analysis of Transmission Line with 3 Level SVPWM Based STATCOM for Reactive Power Management

S.M.Padmaja [#1], N Silpa[#2]
[#1]Professor, Department of Electrical & Electronics Engineering
[#2]Asst. Professor, Department of Computer Science & Engineering
Shri Vishnu Engineering College for Women
Bhimavaram, Andhra Pradesh, India

Abstract

The occurrence of sudden faults in a power transmission network leads to severe short term imbalance in the power system stability. Without threatening the power system stability, the power transfer capability of a transmission network can be enhanced to its maximum limits by using Flexible AC Transmission System (FACTS) controllers. The application of FACTS technology through multilevel converter topologies is attracting research interests due to its additional benefits in improving the power quality. Therefore, appropriate fault analysis for a reliable multilevel converter is the prerequisite for the realization of transmission network.

This paper is intended to investigate the voltage profile and reactive power prevailing in the transmission network of IEEE-14 bus system during the weakest period of the line to ground fault. The performance of traditional 2-level voltage source converter is compared with that of 3- level diode clamped multilevel converter topology through an efficient Space Vector Pulse Width Modulation (SVPWM) control strategy. The complete fault analysis is verified through the simulation in MATLAB / SIMULINK.

Keywords*: 3-SVPWM, STATCOM, Multi Level Converter, Reactive Power Management, L-G Fault.*

I. INTRODUCTION

Line to Ground faults are most popular and commonly occurs in power transmission and distribution networks [1-2]. The faults involve with varying amounts of impedance. A fault with zero ground impedance is termed as short circuit with maximum fault current. Whereas, many faults are with varying ground impedance and decides the severity of the fault [3]. Various protection schemes have been involved for the safety of the equipment [4-5]. However, the most critical requirement for electrical power utilities is an uninterruptible and continuous power flow. Therefore, analysis of the faulted power system and its influence in terms of extent of voltage sag and reactive power availability is necessary for the stable, safe and secured power system. Such demands can be met by the by the new configured applications of power electronics known as FACTS. The instantaneous voltage support and improvement of the transient stability by reactive power exchange with the power system is achieved through a Static Synchronous Compensator (STATCOM) application from FACTS family [6-7]. The STATCOM has inherent potential in giving faster response and greater output to a system with depressed voltage. For medium voltage and high power applications, reliability is a major concern and thus the concept of multilevel converters have been developed that produce a synthesized stair case voltage waveform. Compared to conventional two-level VSC, a 3-level diode clamped multilevel converter (DCMC) exhibits a promising converter topology for STATCOM applications [8-9].

The most effective way to operate the power switching devices of the 3-level STATCOM is through the implementation of SVPWM control strategy. In SVPWM technique, the combined effect of all the three output voltages of the STATCOM at the point of common coupling are considered in generating the Pulse Width Modulated switching pattern [10-11]. This unique feature helps in the complete utilization of DC voltage of the STATCOM unlike with other PWM techniques.

In this paper SVPWM control scheme is implemented on 2-level VSC and 3-level DCMC based STATCOM for the case of single line to ground fault on an IEEE-14 bus system under non linear load conditions. The bulk power systems like IEEE-14 bus network need active power flow control also for better performance along with reactive power control. So the authors in this paper concentrated on both the STATCOM and Multi Level STATCOM integrated with and without energy storage device. As case one, the STATCOM is chosen to be optimally located at bus-14 with the fault at bus-3 and their simultaneous impact on all other buses is analyzed [15-16]. In case two, the fault is considered near the STATCOM in the line 12-13. The

IEEE-14 bus system with its standard data is shown figure 1.

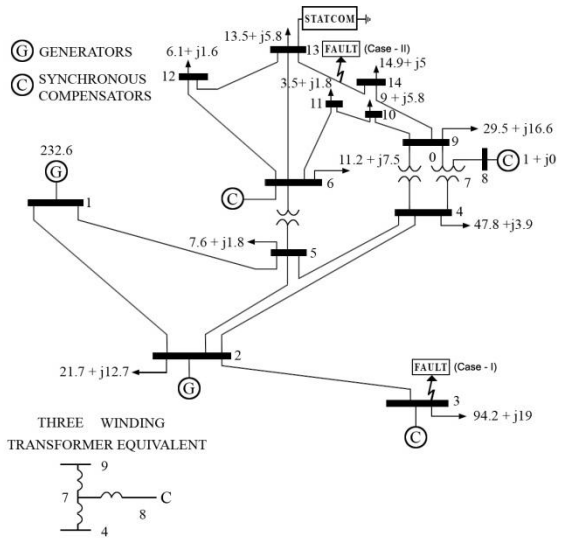

Figure 1. IEEE 14 – Bus System

II. STATCOM MODEL

The STATCOM is generally connected to an AC utility bus by means of a coupling phase shifting transformer. The other side of the STATCOM is connected to a capacitor that carries the DC voltage Vdc. The STATCOM balances the output three phase sinusoidal voltages by maintaining the power equality constraint on both sides [12-13]. A loop equation is written involving the AC side phase voltages and the internal STATCOM series resistance and leakage inductance of the coupling transformer [14].

$$e_{abcs} = R_s i_{abcs} + L_s \frac{d}{dt}(i_{abcs}) + V_{abcl} \qquad (1)$$

Where e_{abcs}, V_{abcl}, i_{abcs} are the three phase quantities expressed as [3x1] matrices and R_s, L_s, are the diagonal matrices as shown below.

$$e_{abcs} = \begin{bmatrix} e_{as} \\ e_{bs} \\ e_{cs} \end{bmatrix};$$

$$V_{abcl} = \begin{bmatrix} v_{al} \\ v_{bl} \\ v_{cl} \end{bmatrix};$$

$$i_{abcs} = \begin{bmatrix} i_{as} \\ i_{bs} \\ i_{cs} \end{bmatrix}$$

Where, $R_s = \begin{bmatrix} R_s & 0 & 0 \\ 0 & R_s & 0 \\ 0 & 0 & R_s \end{bmatrix}$ and

$$L_s = \begin{bmatrix} L_s & 0 & 0 \\ 0 & L_s & 0 \\ 0 & 0 & Ls \end{bmatrix}$$

The AC output of the STATCOM (neglecting harmonics) is expressed in terms of DC voltage as given in equation (2),

$$\begin{bmatrix} e_{as} \\ e_{bs} \\ e_{cs} \end{bmatrix} = \frac{1}{\sqrt{3}} M \; v_{dc} \begin{bmatrix} \sin\theta(t) \\ \sin(\theta(t) - \frac{2\pi}{3}) \\ \sin(\theta(t) + \frac{2\pi}{3}) \end{bmatrix} \qquad (2)$$

Where, $\theta(t) = \omega t + \alpha$

M and θ are the amplitude modulation Index (M.I) and angle modulation index respectively.

vdc is the DC bus voltage and ω is the system frequency.

The dynamic response of the STATCOM is proportional to the real and reactive power exchange between the STATCOM and the utility system which is controlled through the direct (Id) and quadrature axis (Iq) current components respectively. Thus, it is desirable to transfer the parameters in the abc frame to the dqo frame through the transformation matrix k [10] as given in equation (3).

$$K = \frac{2}{3} \begin{bmatrix} \cos\theta_s & \cos(\theta_s - \frac{2\pi}{3}) & \cos(\theta_s + \frac{2\pi}{3}) \\ \sin\theta_s & \sin(\theta_s - \frac{2\pi}{3}) & \sin(\theta_s + \frac{2\pi}{3}) \\ 1/2 & 1/2 & 1/2 \end{bmatrix} \qquad (3)$$

The DC side circuit of the STATCOM is expressed as,

$$\frac{d}{dt}\left(\frac{v_{dc}}{2}\right) = \frac{1}{C}(i_{dc}) \quad (4)$$

The DC current idc is related to AC phase currents [iabcs] at the STATCOM terminal.

$$i_{dc} = -\frac{1}{\sqrt{3}} M \begin{bmatrix} i_{as} \\ i_{bs} \\ i_{cs} \end{bmatrix} \begin{bmatrix} \sin\theta_m \\ \sin(\theta_m - \frac{2\pi}{3}) \\ \sin(\theta_m + \frac{2\pi}{3}) \end{bmatrix} \quad (5)$$

The d and q axis voltage equations of the STATCOM connected at the AC side load terminals are shown in equations (6) and (7) in which the d and q current components are also coupled.

$$v_{ds} = v_{ml} + R_s i_{ds} + L_s \frac{d}{dt}(i_{ds}) - L_s \omega_{iqs} \quad (6)$$

$$v_{qs} = R_s i_{qs} + L_s \frac{d}{dt}(i_{qs}) + L_s \omega_{ids} \quad (7)$$

Based on above equations (6) and (7), the amplitude and angle modulation index of the resultant vector are calculated from equations (8) and (9),

$$M = \frac{\sqrt{3}}{v_{dc}} \sqrt{v_{ds}^2 + v_{qs}^2} = \frac{\sqrt{3}}{v_{dc}} V_{ref} \quad (8)$$

$$\alpha = \tan^{-1} \frac{v_{qs}}{v_{ds}} \quad (9)$$

III. SVPWM CONTROL STRATEGY

The SVPWM control methodology is extended from a traditional 2-level STATCOM to a 3-level diode clamped multilevel converter based STATCOM. SVPWM control scheme creates an efficient gate pulse pattern for multilevel converter. A reference space vector is generated from the combined effect of three phase output voltages to create the desired sinusoidal shaped waveform. SVPWM technique is made suitable for high voltage and high power application as it shows relatively good utilization of the DC link voltage. However, as the number of levels increase, the redundancy with the switching state increases. So it is important to balance between losses and the selection of multilevel converter levels for certain applications. The SVPWM technique alleviated for higher levels is same as the basic implementation of SVPWM in 2-level VSC[11]. The steps involved for the determination of resultant reference voltage vector shown in Figure 2 is discussed in section II. The magnitude and angle of the reference space vector voltage is obtained from the parks transformation of 3Ø-2Ø conversion and its amplitude and angle modulation index are obtained from equations (8) and (9).

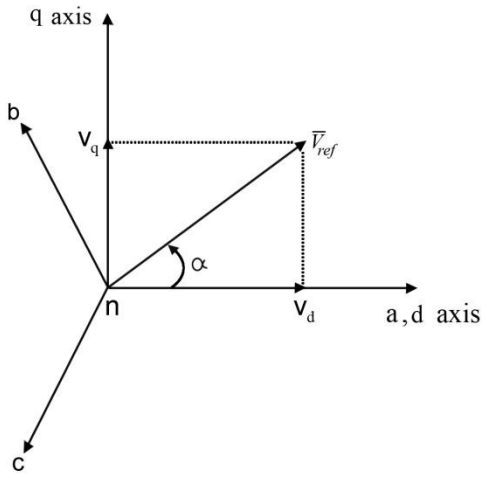

Figure 2. Reference Voltage Space Vector

A. Switching States

In a two level VSC, the number of switching devices in each leg of the converter is two, due to which the total possible switching voltage vectors are 2^3=8 obtained from eight different switching combinations. Out of which two are zero vectors and six are active vectors.

In a 3-level VSC, the number of switching devices in each leg of the converter is double that of in 2-level VSC, due to which there are three different switching states for each leg and so the total number of switching voltage vectors possible are 3^3 = 27. With this advantage SVPWM aims to identify the nearest voltage vectors closer to the reference space vector. The three closest vectors of the commanded reference vector Vref, are usually used to synthesis V_{ref}.

The three different switching states denoted as 1, 0 and -1 developed three levels of resultant line voltages as $1/2V_{dc}$, 0, $-1/2V_{dc}$. The 27 voltage vectors are classified into four groups as 3 zero voltage vectors, 12 small vectors, 6 large vectors and 6 medium voltage vectors as shown in the Table 1.

The space vector V_0 is a zero vector with magnitude '0' obtained from three types of switching combinations (1 1 1), (0 0 0), (-1 -1 -1). Certain switching combinations like V_1: (1 0 0), (0 -1 -1); V_2 : (1 1 0), (0 0 -1); V_3 : (0 1 0), (-1 0 -1); V_4 : (0 1 1), (-1 0 0); V_5 : (0 0 1), (-1 -1 0); V_6 : (1 0 1), (0 -1 0); produce a magnitude of 1/3 V_{dc} and considered as small vectors.

Each small vector is obtained from two different switching combinations. The voltage vectors with magnitude 2/3 Vdc come under large vectors obtained from the switching combinations V_7: (1 -1 -1); V_9: (1 1 -1); V_{11}: (-1 1 -1); V_{13}: (-1 1 1); V_{15}: (-1 -1 1); V_{17}: (1 -1 1).

$\frac{1}{\sqrt{3}}V_{dc}$ is the magnitude of medium vector which is midway between small and large vectors obtained from the switvhing combinations of V8 : (1 0 -1); V10 : (0 1 -1); V12 : (-1 1 0); V14 : (-1 0 1); V16 : (0 -1 1); V18 : (1 -1 1).

Table 1. Magnitude of 27 Voltage Vectors and Their Switching State

No. of Switching state	Switching State			Space Vector	Angle	Vector Type	Magnitude	No. of Switching combinations
1	1	1	1	V_0	0	Zero	0	3
2	0	0	0					
3	-1	-1	-1					
4	1	0	0	V_1	0	Small Vector	$\frac{1}{3}V_{dc}$	2
5	0	-1	-1					
6	1	1	0	V_2	$\frac{\pi}{3}$		$\frac{1}{3}V_{dc}$	2
7	0	0	-1					
8	0	1	0	V_3	$\frac{2\pi}{3}$		$\frac{1}{3}V_{dc}$	2
9	-1	0	-1					
10	0	1	1	V_4	π		$\frac{1}{3}V_{dc}$	2
11	-1	0	0					
12	0	0	1	V_5	$\frac{4\pi}{3}$		$\frac{1}{3}V_{dc}$	2
13	-1	-1	0					
14	1	0	1	V6	$\frac{5\pi}{3}$		$\frac{1}{3}V_{dc}$	2
15	0	-1	0					
16	1	-1	-1	V7	0	Large Vector	$\frac{2}{3}V_{dc}$	1
17	1	1	-1	V9	$\frac{\pi}{3}$		$\frac{2}{3}V_{dc}$	1
18	-1	1	-1	V11	$\frac{2\pi}{3}$		$\frac{2}{3}V_{dc}$	1
19	-1	1	1	V13	π		$\frac{2}{3}V_{dc}$	1
20	-1	-1	1	V15	$\frac{4\pi}{3}$		$\frac{2}{3}V_{dc}$	1
21	1	-1	1	V17	$\frac{5\pi}{3}$		$\frac{2}{3}V_{dc}$	1
22	1	0	-1	V8	$\frac{\pi}{6}$	Medium Vector	$\frac{1}{\sqrt{3}}V_{dc}$	1
23	0	1	-1	V10	$\frac{\pi}{2}$		$\frac{1}{\sqrt{3}}V_{dc}$	1
24	-1	1	0	V12	$\frac{5\pi}{6}$		$\frac{1}{\sqrt{3}}V_{dc}$	1
25	-1	0	1	V14	$\frac{-5\pi}{6}$		$\frac{1}{\sqrt{3}}V_{dc}$	1
26	0	-1	1	V16	$\frac{-\pi}{2}$		$\frac{1}{\sqrt{3}}V_{dc}$	1
27	1	-1	1	V18	$\frac{-\pi}{6}$		$\frac{1}{\sqrt{3}}V_{dc}$	1

B. Space Vector Diagram

The 27 space voltage vectors are represented in a hexagon plane formed by 6 sectors, with each sector sub divided into 4 regions 1, 2, 3 and 4 as shown in Figure 3. For example, if the reference vector is in sector 1 and region 3, the three nearest voltage vectors are V1, V2 and V8. V1 is obtained with a two different switching states i.e., (100), (0-1-1). Similarly V2 is obtained with (00-1)(110) and V8 by the voltage vector (10-1). That means there exists different switching states for the same voltage level as for the case of V0 and V2. Such non-zero vectors are called small vectors pointing to the vertices of the inner hexagon. The three phase voltage levels obtained from the non-zero voltage vectors are $\frac{2}{3}$Vdc, $\frac{1}{\sqrt{3}}$ Vdc and $\frac{1}{3}$Vdc.

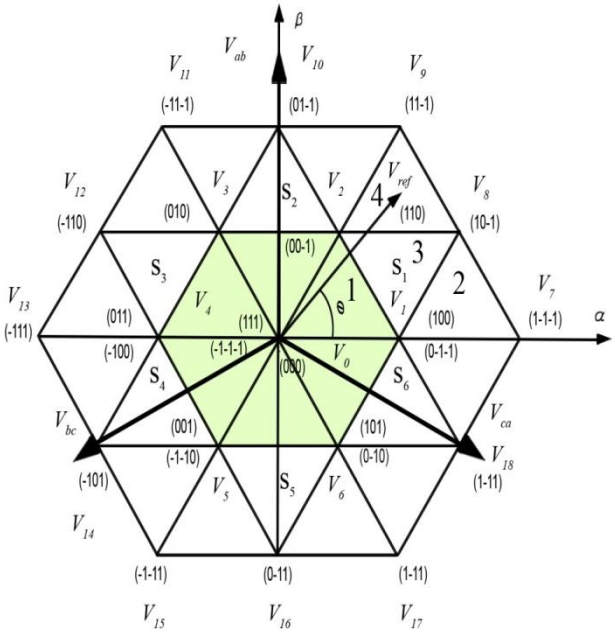

Figure 3. Switching state vectors of 3 –level VSI represented in Hexagon model

C. Determination of Sector and Region

The position of the reference vector in any sector is identified by the angle modulation index similar to that of 2-level VSC. To identify the region of a sector in which the reference vector is placed, a simple vector resolution calculation is followed as discussed below. In Figure 4 each side of the region is considered as unity and the reference vector m_n is resolved into m_1 and m_2. The phasor resolution is re-presented in Figure 5. Based on the magnitude of m_1 and m_2, the placement of the reference vector is determined. Relevant equations for the calculation of m_1 and m_2 are discussed below.

$$\frac{p}{\sin\frac{\pi}{2}} = \frac{q}{\sin\frac{\pi}{3}} \quad (10)$$

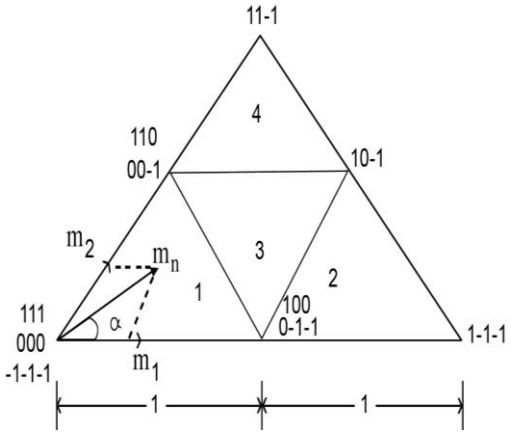

Figure 4. Reference vector in region 1 of sector 1

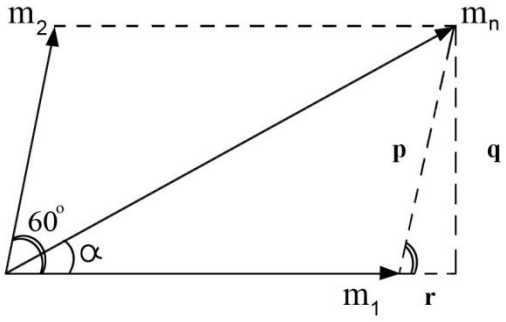

Figure 5. Phasor resolution of reference vector

$$p = m_2 = q\frac{2}{\sqrt{3}} = \frac{2}{\sqrt{3}} m_n \sin\alpha \quad (11)$$

$$\therefore m_2 = \frac{2}{\sqrt{3}} m_n \sin\alpha \quad (12)$$

$$m_1 = m_n \cos\alpha - r \quad (13)$$

$$m_1 = m_n \cos\alpha - p\cos\frac{\pi}{3} \quad (14)$$

$$m_1 = m_n \cos\alpha - [(\frac{2}{\sqrt{3}} m_n \sin\alpha)\cos\frac{\pi}{3}] \quad (15)$$

$$\therefore m_1 = m_n (\cos\alpha - \frac{\sin\alpha}{\sqrt{3}}) \quad (16)$$

Based on the values obtained for m1 and m2 from equations (24) and (28), the region for the location of

reference vector is identified from the conditions shown in Table 2.

Table 2. Conditions for the Location Reference Vector

Condition	Region
$m_1 \leq 1$ $m_2 \leq 1$ $m_1 + m_2 \leq 1$	1
$m_1 > 1$	2
$m_2 \leq 1$ $m_2 \leq 1$ $m_1 + m_2 > 1$	3
$m_2 > 1$	4

D. ON Tme of the Reference Vector in a Region

The ON time of the reference vector in any region of a sector is calculated by applying the volt-time rule to the three nearest voltage vectors with their respective switching times. Consider the reference vector in sector 1 and region 3 as shown in Figure 6. V_1, V_2 and V_8 are the nearest voltage vectors with their respective switching times as T_a, T_b and T_c. Equation (17) shows the volt-time balance relationship with the respective nearest vectors values. Since V_1, V_2 voltage vectors are available with two switching states, proper switching pattern is followed such that, only one device operates during the switching transition from one state to other. From the switching pattern, the switching time for each switch can be determined.

$$V_1T_1 + V_2T_2 + V_8T_3 = V_{ref}T_S \qquad (17)$$

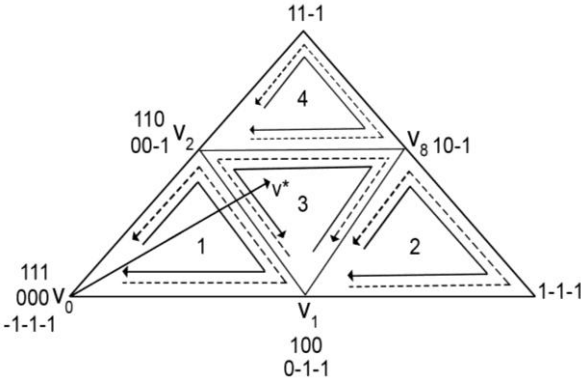

Figure 6. Selection of the Sequence of voltage vectors in each region

The amplitude and the angle of the voltage vectors V1, V2, V8 are substituted from the table xx

$$\frac{1}{3}V_{dc}T_a + \frac{1}{\sqrt{3}}V_{dc}\left(\cos\frac{\pi}{6} + j\sin\frac{\pi}{6}\right)T_b + \frac{1}{3}V_{dc}\left(\cos\frac{\pi}{3} + j\sin\frac{\pi}{3}\right)T_c = V_{ref}(\cos\theta + j\sin\theta)T_s \qquad (18)$$

Dividing the equation (18) into real and imaginary parts eases the calculations for the duty cycle.

Equating the real parts,

$$\frac{1}{3}V_{dc}T_a + \frac{1}{2}V_{dc}T_b + \frac{1}{6}V_{dc}T_c = V_{ref}\cos\theta T_s \qquad (19)$$

Multiplying above equation with $\frac{3}{V_{dc}}$

$$T_a + \frac{3}{2}T_b + \frac{1}{2}T_c = 3\frac{V_{ref}}{V_{dc}}\cos\theta T_s \qquad (20)$$

Equating the imaginary parts,

$$\frac{1}{\sqrt{3}}\frac{1}{2}V_{dc}T_b + \frac{1}{3}\frac{\sqrt{3}}{2}V_{dc}T_c = V_{ref}\sin\theta T_s \qquad (21)$$

Multiplying above equation with $\frac{3}{V_{dc}}$

$$\frac{\sqrt{3}}{2}T_b + \frac{\sqrt{3}}{2}T_c = 3\frac{V_{ref}}{V_{dc}}\sin\theta T_s \qquad (22)$$

The uniform distribution of sampling time is expressed as

$$T_S = T_a + T_b + T_c \qquad (23)$$

By solving equations (20), (22) and (23), we get

$$T_a = T_S[1 - 2M\sin\theta] \qquad (24)$$

$$T_b = T_S\left[2M\sin\left(\frac{\pi}{3}+\theta\right) - 1\right] \quad (25)$$

$$T_c = T_S\left[1 - 2M\sin\left(\frac{\pi}{3}+\theta\right)\right] \quad (26)$$

Where M is the Modulation index and expressed as,

$$M = \sqrt{3}\frac{V_{ref}}{V_{dc}} \quad (27)$$

The time duration of reference vector in remaining regions of all the sectors is calculated in the similar fashion. The optimal switching pattern followed in each region is represented with respect to the ON time durations of respective switching vectors T_a, T_b, and T_c in that region. Figure 7 depicts the demanded states of the upper switches of one phase S_{1a} & S_{2a} corresponding to T_a, T_b, T_c, in region 3 of sector 1. However, the switching states of lower switches in each phase are complement to that of their upper switches. Similar procedure is applied to decide the total switching time of each switch in the remaining regions of all the sectors. The method of generating of PWM pulses is the same as that in 2-L SVPWM. The total ON time of each switch in each region over a sampling time TS is compared with a triangle carrier to generate the SVPWM pulses.

IV. PERFORMANCE EVALUATION

In this paper, the effect of SVPWM controlled 2-Level and 3-Level DCMC based STATCOM on the stability of the power system during the line-ground fault is demonstrated. As a test model, a standard IEEE-14 bus system is considered to evaluate its performance. The optimum locations for the placement of STATCOM are chosen as the buses with least voltage and that provide minimum losses [15-16]. Figure 1 shows the single line diagram of the IEEE-14 bus system integrated with 138KV and 100MVA STATCOM at bus-14. Two cases of location of line to ground fault is considered. One is far away at bus -3 abd other is near to bus -14 in the middle of the line 13-14, with a fault impedance of 50Ω. The digital simulation using PSB/ Simulink was performed. The simulation results of 2 level and 3 level STATCOM reactive current components, DC capacitor voltages, transmission line voltages, active and reactive powers and load voltages at all the buses are analyzed during the fault.

Case I: At t=0.1s to 0.12s, for the sudden line-ground fault at bus-3, the system becomes weak and the bus voltages exhibit oscillations and a high reactive power is drawn instantaneously towards bus-3. The sudden supply of adequate real and reactive power transfer in the lines near to bus-3 is adjusted with the sacrifice of a little voltage in order to maintain the system stable. Since the STATCOM is not supported by any energy storage device and is placed far away at weak bus-14, it is not feasible to supply adequate reactive power from the STATCOM through all the lines towards bus-3. But, it helps in the increase of required reactive power drawn towards bus-3 with decrease in active power in the lines connected to bus-3. As the source is near to the fault compared to the location of STATCOM, the active and reactive powers are drawn from the nearby buses to maintain the stability of the system.

In this process there is an instantaneous dip in voltage at the starting of the fault and with the impact of STATCOM at bus-14, there is quick recovery of the voltage without losing the stability of the system. However, if the STATCOM is located at the vicinity of bus-3 itself, the amount of disturbance in voltage, real and reactive power transfer is reduced. The dynamic and stable response of the 3-level DCMC STATCOM manages the active and reactive powers and regulates the voltage in comparatively lesser time as shown. The impact of STATCOM on all the 14 bus voltages is depicted in Table 3.

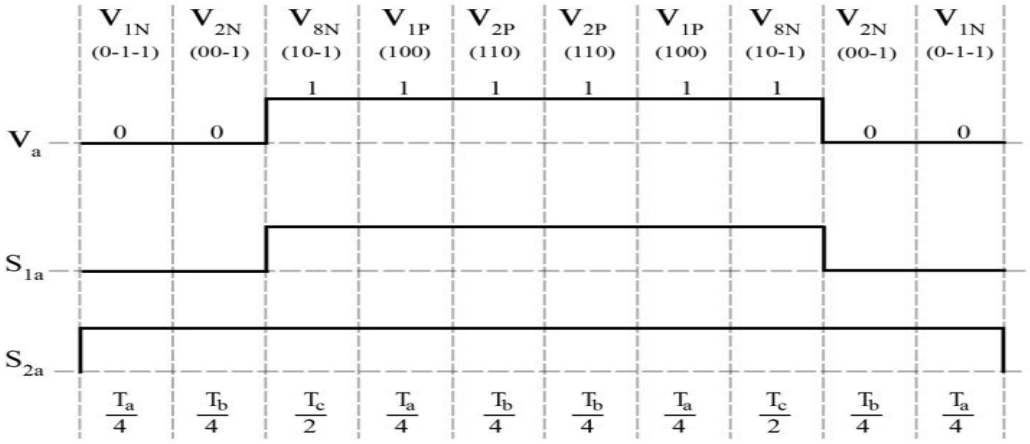

Figure 7. Switching pattern for phase A voltage and demanded status of S_{1a} and S_{2a}

Table 3 . Bus Voltage During the Fault with and without 2 Level and 3 Level SVPWM statcom

BUS NO.	Without STATCOM	2LSVP STATCOM	3LSVP STATCOM
1	0.979	0.965	0.95
2	0.95	0.938	0.928
3	0.88	0.868	0.869
4	0.913	0.905	0.91
5	0.92	0.914	0.914
6	0.964	0.96	0.96
7	0.95	0.944	0.948
8	0.975	0.961	0.968
9	0.946	0.941	0.945
10	0.941	0.938	0.94
11	0.95	0.942	0.944
12	0.95	0.95	0.954
13	0.949	0.95	0.958
14	0.934	0.97	0.99

Figure 8 shows that the load voltage at bus-14 drops sharply and then slowly settles towards its normal value. Therefore, the STATCOM injects reactive power and that drawn from the source buses1 and 2 through the neighboring lines towards bus-14 is reduced. Comparatively 3-level SVPWM STATCOM shows dynamic and fast response in settling the voltage dip to its normal value during the fault.

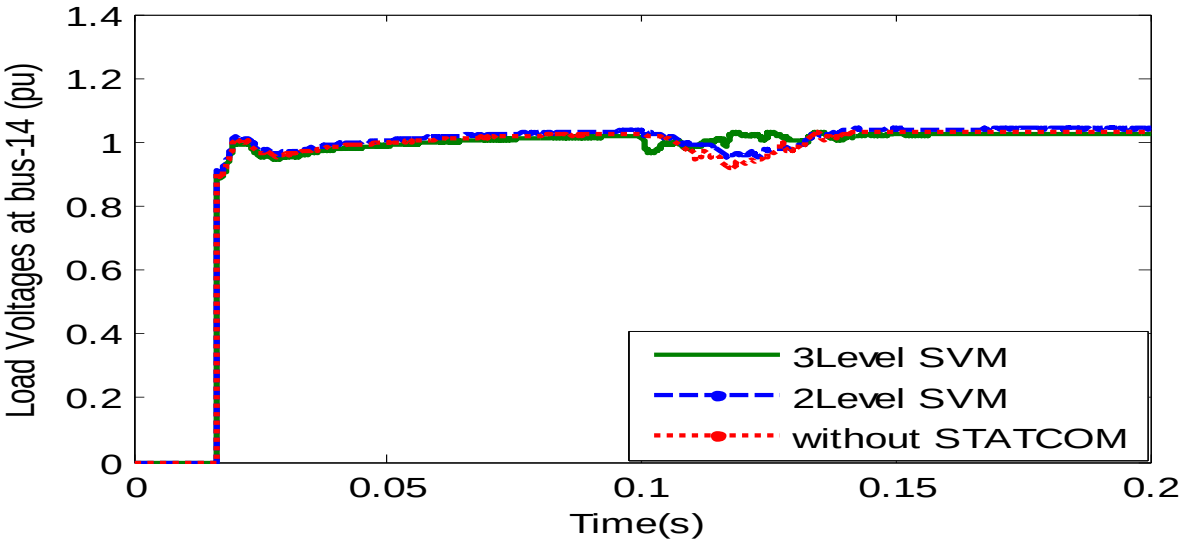

Figure 8. Comparison of load voltages at bus14 without and with 2-Level and 3-Level STATCOM

The DC side capacitors for 2-level and 3-level STATCOMs considered in this paper are not supported by any energy storage devices. So the capacitors draw some power from the bus system for their charging. It is observed from Figure 9 that at t=0.1s, Vdc drops momentarily, that means the real power flows from the DC capacitor to the transmission line.

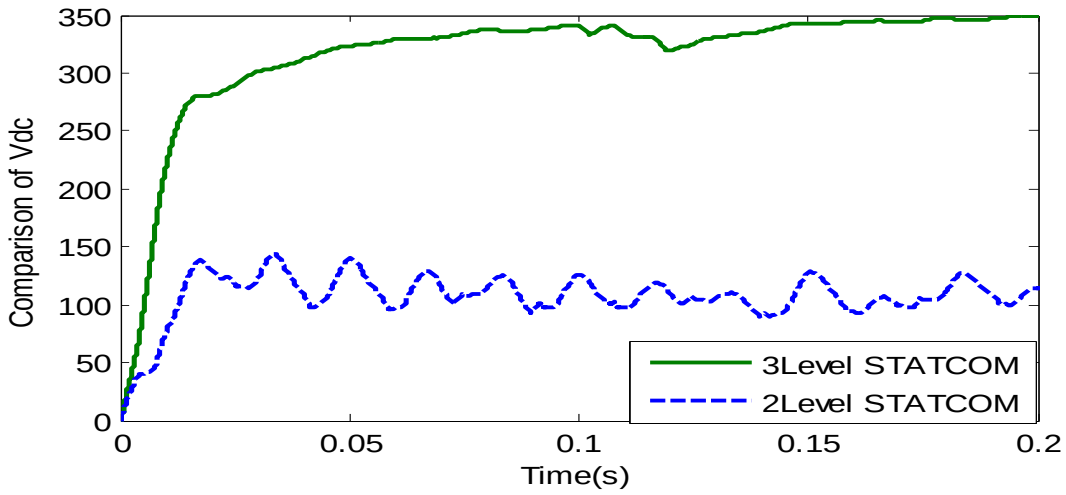

Figure 9. Comparison of DC capacitor voltages of 2-Level and 3-Level STATCOM

Figure 10 and figure 11 shows the variations of reactive current components of the STATCOM and the utility system that is responsible for the fast compensation of the reactive power and stabilization of the voltage. It is observed that 3-Level SVPWM is giving far better compensation compared to 2-Lvel SVPWM. The comparison of the variations of voltages, active and reactive powers in all the lines are shown in Table 4. It is observed that the line and bus voltages at and near bus 14 are improved. The lines 9-14 and 13-14 that are connected to bus 14 are more benefitted with an increase in voltage profile, increase in active power transfer and decrease in reactive power.

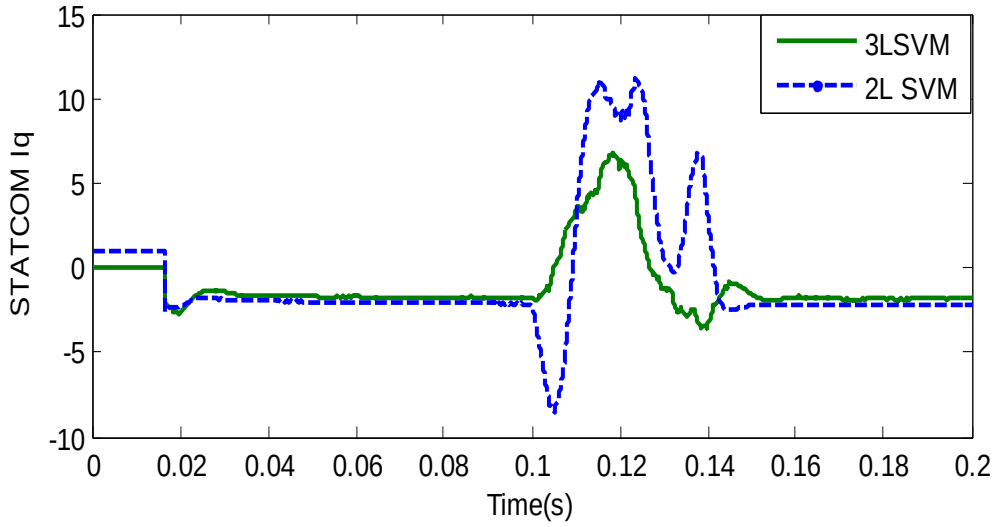

Figure 10. STATCOM reactive current components

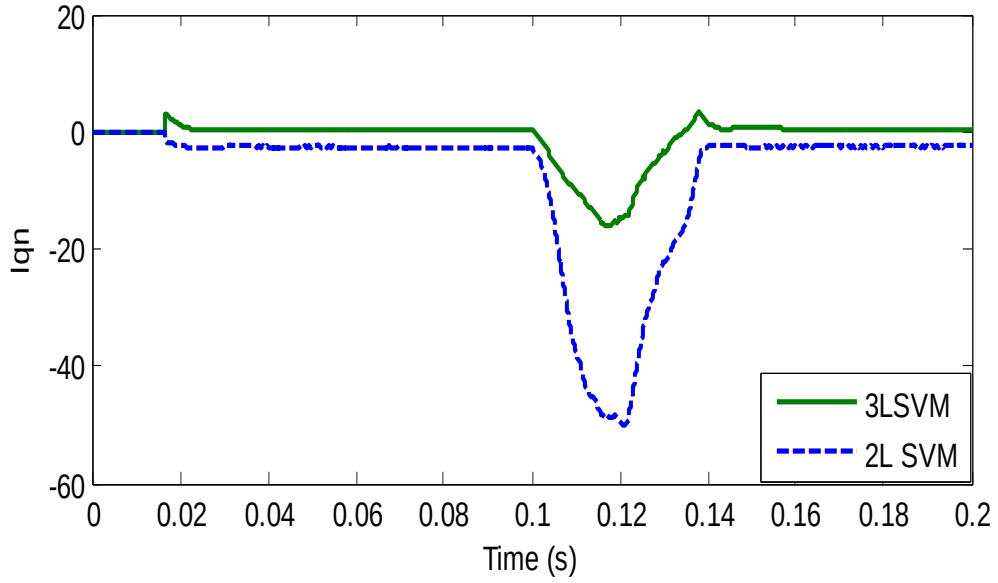

Figure 11. Utility reactive current components

Table 4. Voltage , Active and Reactive powers in All the Lines During the Worst Conditoin of the LG Fault

	Line Voltages			Active Power in MW			Reactive Power in Mvar		
Line No.	without statcom	2-Level	3-Level	without statcom	2-Level	3-Level	Without statcom	2-Level	3-Level
1-2	0.95	0.939	0.95	0.3975	0.40325	0.385	0.16	0.152	0.152
2-3	0.9	0.899	0.9	0.2835	0.26	0.255	0.16	0.172	0.175
1-5	0.934	0.926	0.932	0.212	0.22	0.2212	0.091	0.06975	0.06675
2-5	0.93	0.922	0.928	0.138	0.144	0.1475	0.03225	0.017	0.0187
2-4	0.93	0.922	0.928	0.153	0.16	0.163	0.0335	0.02625	0.0285
3-4	0.9	0.9	0.9	0.142	-0.1	-0.0825	-0.119	-0.165	-0.172

4-5	0.91	0.91	0.91	0.305	0.3105	0.332	0.0786	0.05525	0.0425
7-8	0.952	0.952	0.96	0.012	0.01	0.014	-0.002	-0.005	-0.0002
7-9	0.95	0.95	0.95	0.012	0.0151	0.01595	0.00157	-0.0029	0.00058
6-11	0.95	0.95	0.95	0.035	0.0362	0.0362	0.0189	0.0187	0.0186
6-12	0.95	0.95	0.95	0.0256	0.024	0.027	0.01	0.0062	0.005
6-13	0.95	0.95	0.95	0.06	0.06	0.06	0.0267	0.0107	0.0065
9-10	0.94	0.94	0.948	0.0151	0.014	0.014	0.00035	0.0008	0.003
10-11	0.95	0.95	0.95	-0.021	-0.022	-0.0226	-0.014	-0.014	-0.0135
9-14	0.96	0.96	0.99	0.0187	0.05	0.074	0.0064	0.0049	0.0035
12-13	0.95	0.95	0.955	0.0065	0.0085	0.012	0.0026	-0.00075	-0.00285
13-14	0.95	0.962	0.98	0.0223	0.0275	0.05	0.0122	-0.006	-0.0166

Case II: The line-ground fault is considered at t=0.1 s to o.12 s in the middle of the line 13-14 without changing the position of the STATCOM at bus 14. Here, the STATCOM is considered with the energy storage device to provide performance improvement. Occurrence of a fault suddenly draws large amounts of line currents to satisfy the required reactive power. Compensation of reactive power not only reduces the losses, but also regulates the voltage stability. In the process of controlling active and reactive power flow, in all the lines of the system, a little voltage is needed to be sacrificed without loosing the stability of the system. The impact values of bus voltages and line voltages, active powers and reactive powers by the 2-level and 3-level SVPWM controlled STATCOM during the worst condition of the fault period are tabulated in Table 5 and Table 6. Undoubtedly, there is an improvement of voltage at bus 14 that is at the point of common coupling by 3L DCMC based STATCOM as shown in figure 12.

Table 5. Comparison of Bus Voltages

BUS No.	Without STATCOM	2LSVP at Bus 14	3LSVP at Bus 14
1	0.994	0.975	0.975
2	0.97	0.945	0.955
3	0.9305	0.911	0.93
4	0.9265	0.91	0.91
5	0.93	0.9067	0.911
6	0.974	0.952	0.957
7	0.964	0.94	0.946
8	0.9908	0.9645	0.9725
9	0.96	0.935	0.943
10	0.955	0.93	0.937
11	0.96	0.934	0.94
12	0.95	0.935	0.936
13	0.93	0.928	0.927
14	0.895	0.921	0.94

TABLE 1. COMPARISION OF LINE VOLTAGES, ACTIVE POWERS AND REACTIVE POWERS

	Line Voltage in pu			Active Power in pu			Reactive Power in pu		
Line No	without	2LSVP	3LSVP	without	2LSVP	3LSVP	without	2LSVP	3LSVP
1-2	0.968	0.96	0.958	0.3773	0.3775	0.381	0.15	0.1439	0.14
2-3	0.942	0.928	0.92	0.209	0.203	0.209	0.0875	0.084	0.081
1-5	0.948	0.933	0.93	0.2165	0.245	0.245	0.11	0.1003	0.1

2-5	0.944	0.93	0.925	0.16285	0.184	0.184	0.0668	0.057	0.0568
2-4	0.945	0.93	0.93	0.173	0.19	0.19	0.0643	0.0564	0.055
3-4	0.925	0.91	0.92	-0.0312	-0.017	-0.014	-0.00633	-0.007	-0.0066
4-5	0.919	0.905	0.907	0.257	0.26	0.27	0.067	0.058	0.058
7-8	0.97	0.95	0.96	0.0135	0.013	0.013	-0.0042	-0.0042	-0.0002
7-9	0.9584	0.95	0.95	0.0062	0.009	0.012	0.00687	0.005	0.0056
6-11	0.9545	0.94	0.942	0.03	0.031	0.031	0.0164	0.018	0.0161
6-12	0.95	0.94	0.94	0.0525	0.0563	0.0574	0.033	0.0288	0.0275
6-13	0.9415	0.934	0.932	0.1365	0.165	0.172	0.1635	0.15	0.146
9-10	0.95	0.935	0.94	0.0198	0.016	0.0159	0.0004	0.004	0.004
10-11	0.956	0.95	0.94	-0.0163	-0.0164	-0.0168	-0.0113	-0.0108	-0.0104
9-14	0.923	0.924	0.95	0.07	0.11	0.13	0.112	0.015	0.005
12-13	0.93	0.93	0.93	0.0323	0.039	0.04	0.035	0.028	0.025
13-14	0.865	0.906	0.92	0.0335	0.037	0.045	0.165	0.165	0.164

Also, the reactive power delivered from the source 1 during the fault period is reduced in the presence of the STATCOM at bus 14 of the IEEE System as shown in figure 15. With the analysis on the above results, it is clear that the dynamic performance of the STATCOM in the reactive power compensation during a line-ground fault maintaining the stability of the system. In addition, with a capacitive support at the source and load ends, the performance at all the buses can be still improved.

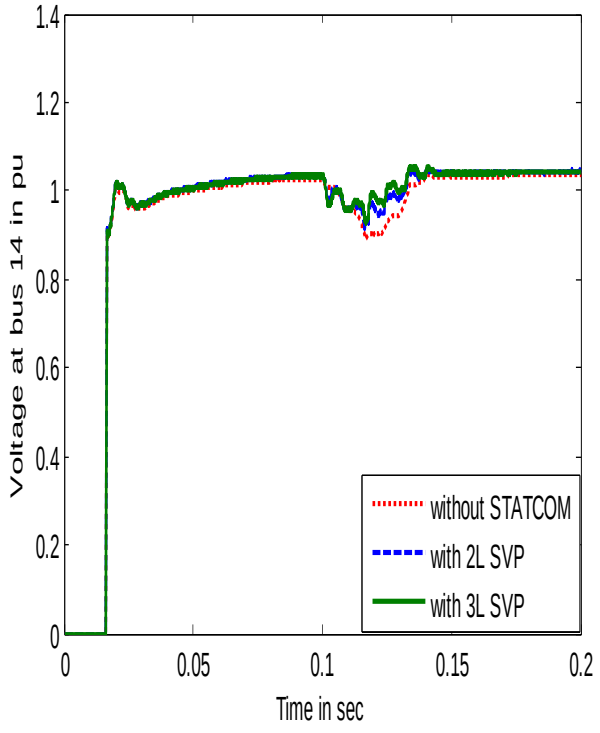

Figure 12. Comparision of voltages at bus 14 under L-G faultin line 13-14

Generally, without STATCOM, for the sudden fault in line 13-14, the neighboring lines carry increased Reactive Power flow obviously drown all through the source, to supply the fault line. With STATCOM a comparative decrease in reactive power flow is observed in the line 9-14 connected to bus-14 as shown in figure 13.

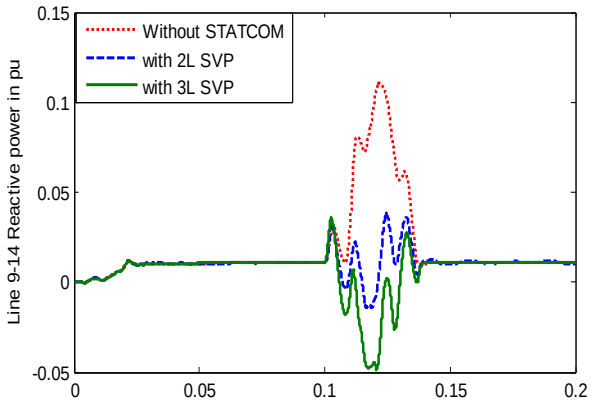

Figure 12. Comparision of reactive power flow in line 9-14

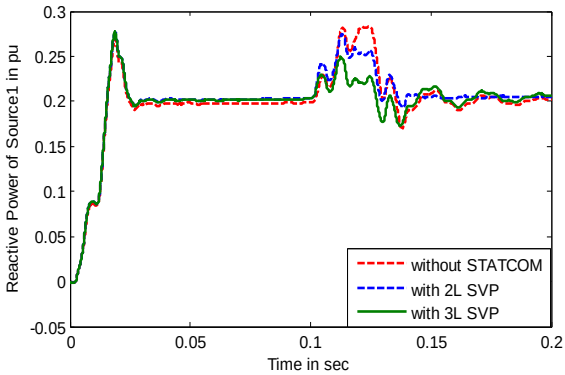

Figure 13. Comparision of reactive power flow in the line 12-13

Simultaneously, it is also observed from figure 14, a comparative decrease in reactive power flow in the line 12-13 which is connected to the faulty line 13-14 through bus 13.

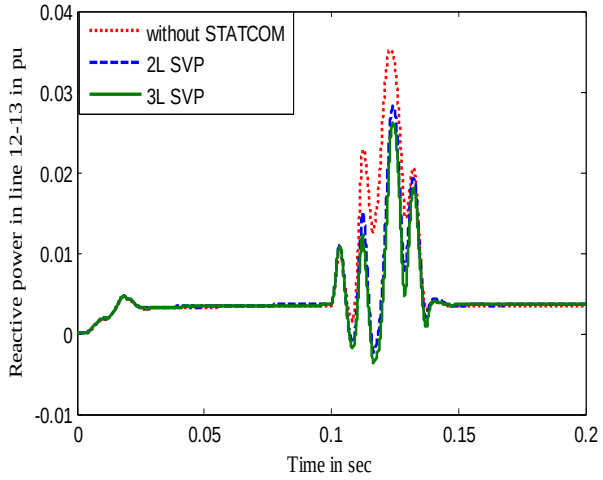

Figure 14. Comparision of reactive power delivered by source 1

The six sectors identified for the location of reference vector with respective alpha variation in SVPWM technique is shown in figure 16. Figure 17 shows the AC output voltage of the 2-level SVPWM controlled voltage source converter which follows the power equality constraint with the DC side capacitor voltage of the STATCOM supported by energy storage device. Similarly, figure 18 shows the three levels of AC output voltage developed by the 3-level SVPWM controlled multi level STATCOM.

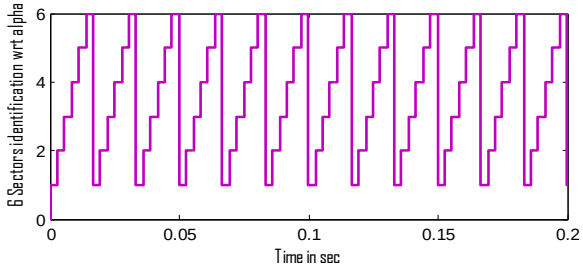

Figure 16. The six sectors identified in SVPWM technique

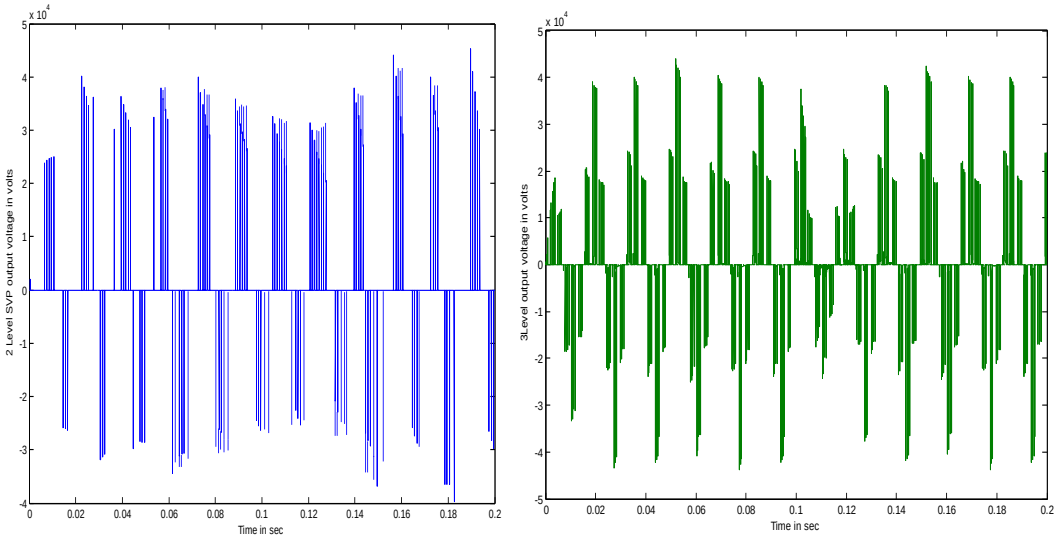

V. CONCLUSION

In this paper a fault compensation strategy is discussed through the implementation of 3-level DCMC and 2-level VSC based STATCOMs on the IEEE-14 bus system. Upon the occurrence of the fault, STATCOM immediately senses the severity of the fault by the error accumulation as the feedback signal. The individual switches of the converter are actively controlled by the SVPWM switching strategy. The threshold value of the error current between the STATCOM and the AC line is the feedback used for the SVPWM controller during the fault period. The effectiveness of the SVPWM controlled 3-Level DCMC is analyzed throughout the fault period in the compensation of reactive power and to allow smooth ride through of the line and load voltages. Highest priority is given to the mitigation of the disturbance due to line-ground fault on the surrounding transmission lines and buses. From the analysis results of the simulation studies, SVPWM controlled 3-level DCMC based STATCOM shows a fault tolerant control strategy to achieve the fast and steady response in managing the

reactive power and voltage profile for the stable operation of the system.

REFERENCES

[1] Dr. Guenter Kiessling, Stefan Schwabe, Dr. Juergen Holbach, "Power System Fault Analysis using Fault Reporting Data of Numerical Relays" Siemens PT&D.

[2] J. Beiza, S. H. Hosseinian and B. Vahidi, "Fault Type Estimation in Power Systems" Iranian Journal of Electrical & Electronic Engineering, Vol. 5, No. 3, Sep. 2009.

[3] M. Sushama, G. Tulasi Ram Das and A. Jaya Laxmi, "Detection of High-Impedance Faults In Transmission Lines Using Wavelet Transform", VOL. 4, NO. 3, MAY 2009 ISSN 1819-6608 ARPN Journal of Engineering and Applied Sciences ©2006-2009.

[4] Yeong Jia Cheng, Eng Kian Kenneth Sng, "Transient Analysis and Fault Compensation During Module Failure in Paralleled Power Modules" IEEE TRANSACTIONS ON INDUSTRY APPLICATIONS, VOL. 42, NO. 2, MARCH/APRIL 2006.

[5] M.Sushama, Dr. G.Tulasi Ram Das, "Detection and Classification of Voltage Sags using adaptive decomposition and wavelet transform" Int.j. Elect.Power Eng.,3(1):2009, Medwell Journals.

[6] N. G. Hingorani and L. Gyugyi, "Understanding FACTS, Concepts, and Technology of Flexible AC Transmission Systems", Piscataway, NJ: IEEE Press, 2000.

[7] Ying Xiao, Y. H. Song, Chen-Ching Liu, Fellow, Y. Z. Sun, "Available transfer capability enhancement using FACTS devices" IEEE Trans. on Power Syst., vol. 18, no. 1, february 2003

[8] K Haritha, S Kumar, Dr.Venugopal, "Design and Operation of an improved hybrid DSTATCOM topology to compensate reactive and harmonics loads" SSRG International Journal of Electrical and Electronics Engineering (SSRG-IJEEE) – volume 2 Issue 3 March 2015

[9] Satish Bhakar, Ahamed Khan, Manish Kumar Bissu, Anurag Singh, "Facts Devices and their Controlling" SSRG International Journal of Electrical and Electronics Engineering (SSRG-IJEEE) – volume 3 Issue 5 May 2016

[10] Tarlochan Singh Sidhu, , Rajiv K. Varma, Pradeep Kumar Gangadharan, Fadhel Abbas Albasri, , and German Rosas Ortiz, "Performance of Distance Relays on Shunt—FACTS Compensated Transmission Lines" IEEE TRANSACTIONS ON POWER DELIVERY, VOL. 20, NO. 3, JULY 2005

[11] Jin-Woo Jung, "Project#2 Space Vector PWM Inverter" Department of Electrical and Computer Engineering, The Ohio State University.

[12] Dong Myung Lee, JinWoo Jung, SangShin Kwak "Simple space vector PWM scheme for three level NPC Inverters including the overmodulation region", Journal of power Electronics Vol.11, No.5, September 2011.

[13] M. S. ElMoursi, Prof. Dr. A. M. Sharaf, "Voltage stabilization and reactive compensation using a novel FACTS- STATCOM scheme" 0-7803-8886-0/05/$20.00 ©2005 IEEE CCECE/CCGEI, Saskatoon, May 2005

[14] Amir H. Norouzi and A. M. Sharaf, "Two Control Schemes to Enhance the Dynamic Performance of the STATCOM and SSSC" IEEE TRANSACTIONS ON POWER DELIVERY, VOL. 20, NO. 1, JANUARY 2005

[15] Maryam Saeedifard, Hassan Nikkhajoei, and Reza Iravani, "A Space Vector Modulated STATCOM Based on a Three-Level Neutral Point Clamped Converter", IEEE TRANSACTIONS ON POWER DELIVERY, VOL. 22, NO. 2, APRIL 2007

[16] M.Arun Bhaskar, M.Mahesh, Dr.S.S.Dash, M.Jagadeesh Kumar, C.Subramani, "Modelling and Voltage Stability Enhancement of IEEE 14 Bus System Using "Sen" Transformer", 2011 International Conference on Signal, Image Processing and Applications, With workshop of ICEEA 2011, IPCSIT vol.21 (2011) © IACSIT Press, Singapoor.

[17] Antonio J. Conejo, Francisco D. Galiana, Ivana Kockar, " Z-Bus Loss Allocation", IEEE transactions on power systems, vol.16, no.1, February 2001.